ELSEVIER

Journal of Alloys and Compounds 330–332 (2002) 292–295

Journal of ALLOYS AND COMPOUNDS

www.elsevier.com/locate/jallcom

Electron microscopy and hydriding properties of $MgYNi_4$ synthesized by mechanical alloying

Yasuyuki Kitano[a,*], K. Yamada[a], M. Miyamoto[a], S. Orimo[b], H. Fujii[b], K. Aono[b], E. Tanabe[c]

[a]*Department of Materials Science, Shimane University, Nishi-Kawatsu 1060, Matsue 690-8504, Japan*
[b]*Faculty of Integrated Arts and Science, Hiroshima University, Kagami-Yama 1-7-1, Higashi-Hiroshima 739-8521, Japan*
[c]*Hiroshima Prefectural Institute of Science and Technology, Higashi-Hiroshima 739-0046-3-10-32, Japan*

Abstract

The ternary alloy, $MgYNi_4$, was synthesized by mechanical alloying (MA). Its microscopic structures and hydriding properties were studied. The annealing of the alloy at 773 K was also studied. The alloy consists of nanocrystals of less than 10 nm in diameter. The capacity of the hydrogen atoms in the alloy increases with the increasing size of the nanocrystals. The crystal structure was found to be the C15 type Laves phase structure for the MA-treated alloy, while crystal structure of the as annealed alloy was the ordered C15 type structure which is conventionally called C15b type and is formally called $AuBe_5$ type structure. The hydrogen capacity in the alloy might have a strong relation to the atomic arrangement of this alloy.

Keywords: Hydrogen storage; Nanostructures; Mechanical alloying; Crystal structure; Transmission electron microscopy

1. Introduction

In order to improve the hydride properties, such as dissolution capacity and hydride or dehydride temperatures, materials in a non-equilibrium state have been intensively investigated. Nanostructured Mg_2Ni alloy synthesized by mechanical alloying (MA) shows a high dissolution capacity — about six or seven times larger than the capacity in the bulk of the same alloy [1,2]. Moreover, the amorphous MgNi alloy, which is also synthesized by the MA-treatment of the Mg_2Ni alloy with additional elemental Ni powders, can contain several times more hydrogen atoms than the nanostructured Mg_2Ni alloy [3]. These alloys were found to be in non-equilibrium states.

The microstructures of some MA-treated Mg–Ni alloys and of several ternary alloys with transition metals has been investigated by electron microscopy [4–8]. In this paper, the microstructures of the ternary alloy, $MgYNi_4$, are reported. Details of the hydrogen properties will be reported elsewhere [9].

2. Experimental

The alloy examined in this work, $MgYNi_4$, was synthesized from the two intermetallic compounds, $MgNi_2$ and YNi_2, by MA [6]. The crystal structures of the two alloys are known to be the Laves phase structure: the former is the $MgNi_2$-type, $hP6_3/mmc$-$(4e)(4f)^2(6g)(6h)$, C36-type structure, and the latter is the $MgCu_2$-type, $cFd3m$-$(8a)(16d)$, C15-type structure. The MA was carried out for 80 h by the use of ball mill machine, Fritsch-P7, with a rotation speed of 400 rpm. After the MA, a heat treatment at 773 K for 600 s was carried out. The microstructures not only of the materials as-MA-treated but also of the as-annealed materials were investigated by electron microscopy. The effects of the heat treatment are also studied.

Since the materials obtained are in the form of micrometer-sized powders, specimens for the electron microscopy are prepared by the focused ion beam technique using an FIB machine (FB2000) [10,11]. The FIB machine is one of the most useful machines for making submicron-sized powders thin enough for electron microscopic observation. An example thinned by the FIB technique is presented in Fig. 1. The Ga ion beam runs from the top left to the bottom right of the figure. The dark irregular part

*Corresponding author. Tel.:/fax: +81-852-32-6402.
E-mail address: kitano@riko.shimane-u.ac.jp (Y. Kitano).

0925-8388/02/$ – see front matter
PII: S0925-8388(01)01531-6

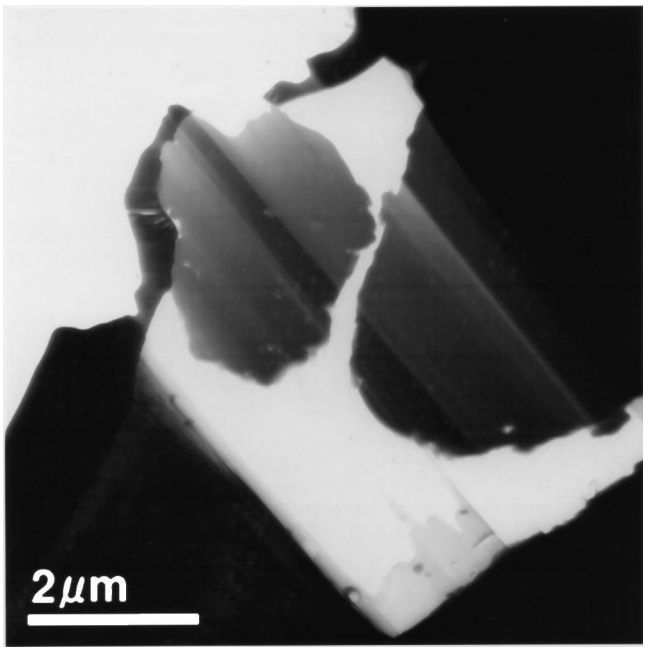

Fig. 1. Example of the TEM specimen prepared by the FIB method.

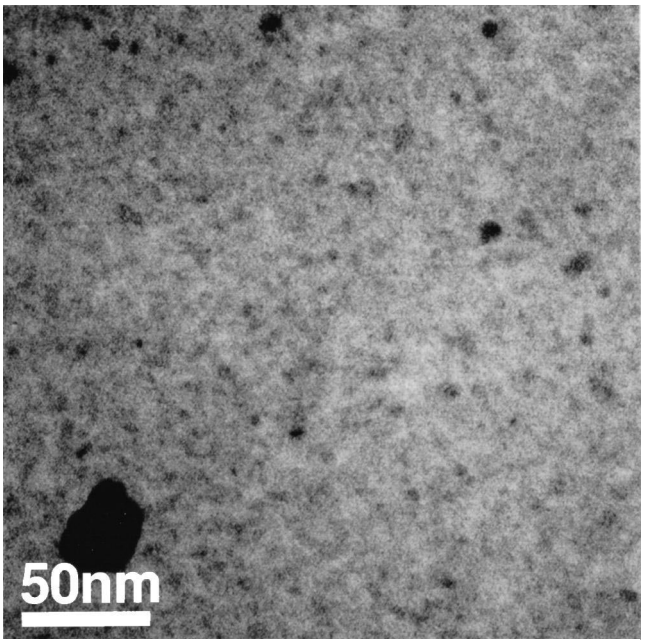

Fig. 2. Bright field images of the MA-treated $MgYNi_4$ alloy. The image contrasts come from the difference in the orientation of the nanocrystals.

seen against the Ga-ion beam is tungsten which has been deposited on the top of the powders in order to protect the direct bombardment of the Ga ions. One powder particle and a half are thinned in Fig. 1. They are mounted in the resin.

The electron microscopes JEM 4000EX and JEM 3000F were employed in this work.

3. Results and discussion

The dissolution capacity of hydrogen atoms was measured to be 0.78 mass% for the MA-treated $MgYNi_4$ alloy. This value corresponds to 0.44 in the ratio (H/M) of hydrogen atom (H) to metal atom (M). In the annealed alloy, the capacity increases up to 0.85 mass% and the ratio H/M to 0.49. A ratio of hydrogen atom to one Mg atom (H/Mg) may be estimated multiplying by six to the ratio H/M. Values of H/Mg, therefore, can be estimated as 2.6 and 2.9 for both materials. Details on the hydrogen properties will be reported elsewhere [9].

An example of electron micrographs using low magnification is presented in Fig. 2 for the 80 h MA-treated $MgYNi_4$ alloy. An example of electron micrographs for the 600 s annealed $MgYNi_4$ alloy is presented in Fig. 3. The contrasts seen in the bright field images result from a difference in the crystallographic orientations. These micrographs show that both alloys are in a state of homogeneous nanostructures. The diameters of the nanocrystals are measured and the statistics are carried out. Histograms of the diameter of the nanocrystals are presented in Fig. 4(a) for the MA-treated alloy and in Fig. 4(b) for the annealed alloy; the average size of the diameters is found to be 5 or 6 nm, and 8 or 9 nm, respectively. Comparing

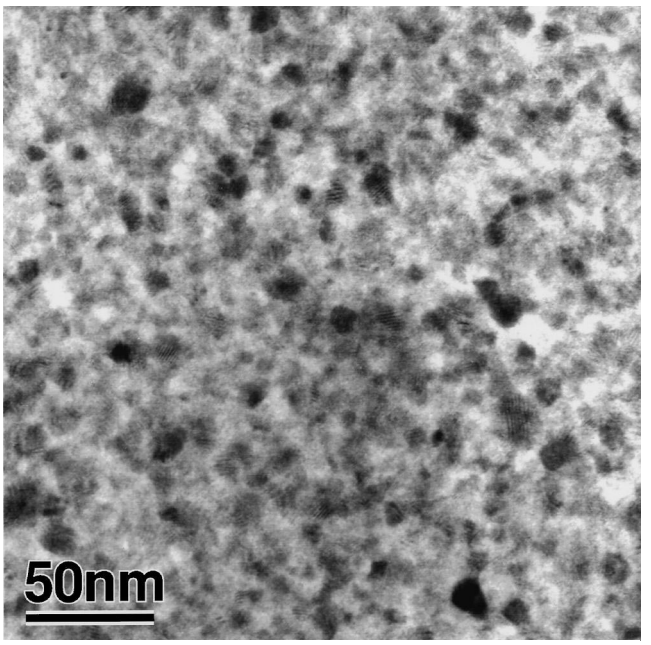

Fig. 3. Bright field images of the annealed $MgYNi_4$ alloy. The image contrasts come from the differences in the orientation of the nanocrystals.

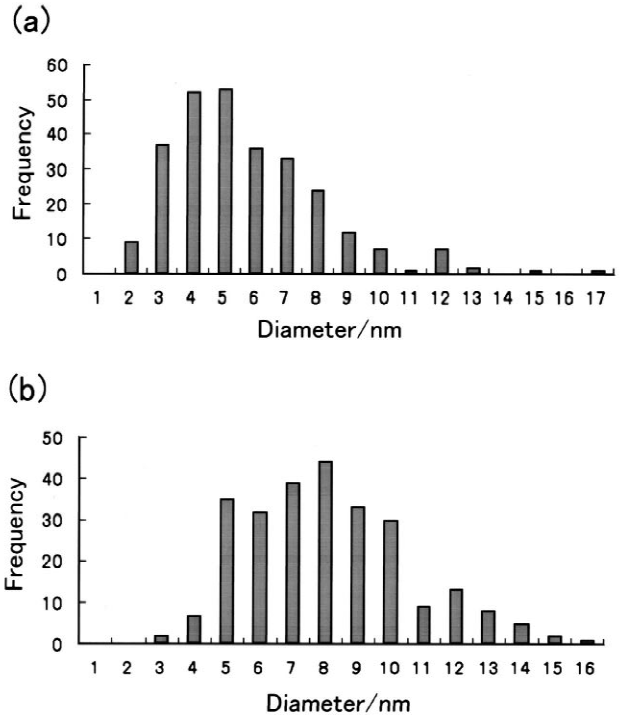

Fig. 4. Histograms of diameter of the nanocrystals measured in the bright field images. (a) Histogram for the MA-treated alloy; the average size is 5 or 6 nm in diameter. (b) Histogram for the annealed alloy; the average size is 8 or 9 nm in diameter.

the size of nanocrystals between these two alloys, crystal growth due to annealing is confirmed.

In high-resolution images, the lattice fringes are clearly seen in the individual nanocrystals. Examples are given in Figs. 5 and 6, corresponding to the MA-treated and annealed alloys, respectively. Boundaries between nanocrystals, however, are not imaged clearly. The specimen thickness and superposition of the nanocrystals might be the reasons for this vagueness.

The electron diffraction patterns of the alloys consist of Debye rings. The Debye rings from the MA-treated materials can be interpreted by the C15-type structure. The diffraction pattern is presented in the upper part of Fig. 7. The Debye rings are rather broad and dull. In the lower part of Fig. 7, the diffraction pattern from the annealed alloy is presented. The Debye rings have become sharp and some new diffraction lines have appeared. These new diffraction lines can be interpreted by the ordering in the C15 Laves phase. This means that the Mg and Y atoms are in the ordered state, occupying the *8a* sites of the space group of $cFd\bar{3}m$ of the C15 type structure. The ordered structure is conventionally called C15b Laves phase and is known to be an $AuBe_5$-type structure, whose space group is $cF\bar{4}3m$-(4*a*)(4*c*)(16*e*).

Probable atomic site for hydrogen have been thought to be the center of a tetrahedral site (T-site) in the Laves phase structure. In the $AuBe_5$-type structure (C15b), a tetrahedron which is made of four atoms, that is, an Mg atom, an Y atom and two Ni atoms, might play an important role.

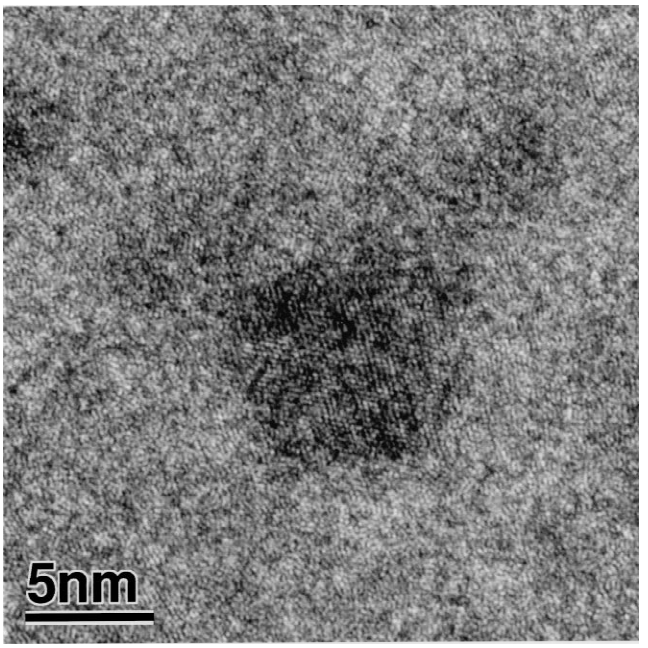

Fig. 5. Example of a high resolution image showing the nanocrystal state of the MA-treated alloy.

4. Conclusion

The ternary alloy, $MgYNi_4$, synthesized by MA is investigated by electron microscopy. The alloy shows a

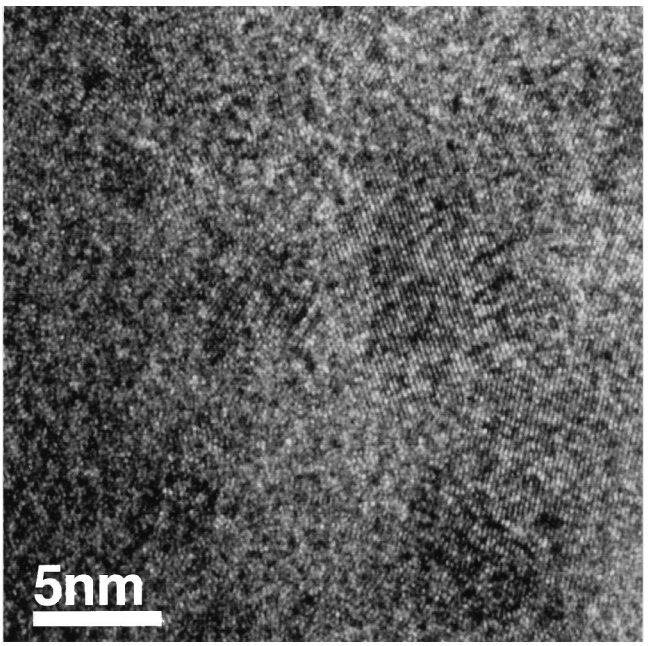

Fig. 6. Example of a high resolution image showing the nanocrystal state of the annealed alloy.

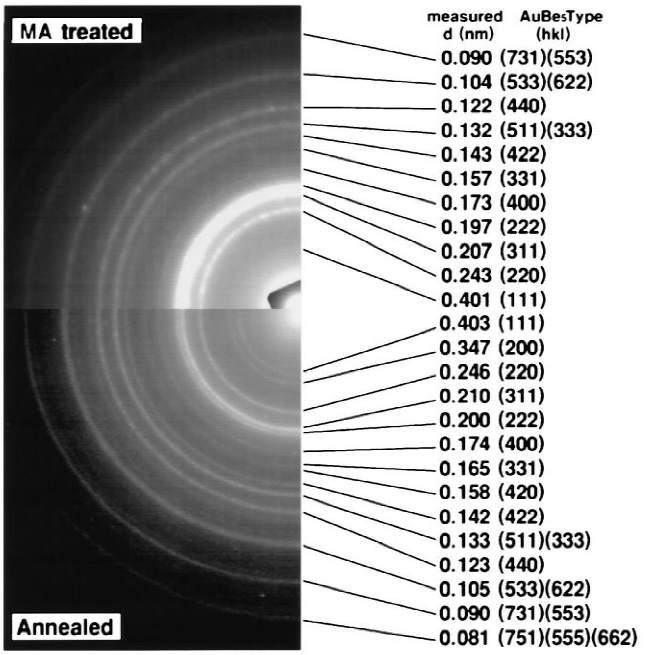

Fig. 7. Electron diffraction patterns of $MgYNi_4$ alloys. The upper side of the diffraction pattern is from the MA-treated alloy, and the lower one is from the annealed alloy. All the Debye rings observed in the upper side are indexed assuming the crystal structure to be the C15 Laves phase. All the Debye rings observed in the lower side are indexed assuming to be the ordered C15b ($AuBe_5$-type) structure. In the upper diffraction pattern, indices 200 and 420 are missing. These two lines are the ordered diffraction lines.

homogeneous state of nanostructure having a size of less than 10 nm in diameter. The hydrogen atom capacity increases with the size of the nanocrystals. Less than three hydrogen atoms per Mg atom are included in the materials.

Acknowledgements

This work is supported by Grant-in-Aid for Scientific Research on Priority Areas(A) 'New Protium Function in Sub-Nano Lattice Matters' (Area No. 299) given by the Ministry of Education, Science and Culture, Japan.

References

[1] S. Orimo, H. Fujii, J. Alloys Comp. 232 (1996) 116–119.
[2] S. Orimo, H. Fujii, K. Ikeda, Acta Mater. 45 (1997) 331–341.
[3] S. Orimo, K. Ikeda, H. Fujii, Y. Fujikawa, Y. Kitano, K. Yamamoto, Acta Mater. 45 (1997) 2271–2278.
[4] Y. Kitano, Y. Fujikawa, N. Shimizu, S. Orimo, H. Fujii, T. Kamino, T. Yaguchi, Intermetallics 5 (1997) 97–101.
[5] K. Yamamoto, Y. Fujikawa, K. Ikeda, S. Orimo, H. Fujii, Y. Kitano, J. Electron Microsc. 47 (1998) 461–470.
[6] K. Yamamoto, S. Orimo, H. Fujii, Y. Kitano, J. Alloys Comp. 293–295 (1999) 546–551.
[7] Y. Kitano, K. Yamada, M. Miyamoto, S. Orimo, H. Fujii, K. Aono, E. Tanabe, Proceedings 12th European Congr. Electron Microscopy, (2000) Vol. II, pp. 47–48.
[8] Y. Kitano, K. Yamada, M. Miyamoto, S. Orimo, H. Fujii, M. Aoki, C. Kawasaki, Proceedings 12th European Congr. Electron Microscopy, (2000) Vol. II. pp. 49–50.
[9] K. Aono, S. Orimo, H. Fujii, J Alloys Comp. submitted for publication.
[10] Y. Kitano, Y. Fujikawa, T. Kamino, T. Yaguchi, H. Saka, J. Electron Microsc. 44 (1995) 410–413.
[11] Y. Kitano, Y. Fujikawa, H. Takeshita, T. Kamino, T. Yaguchi, H. Matsumoto, H. Koike, J. Electron Microsc. 44 (1995) 376–383.